Polymer Chemistry

COMMUNICATION

View Article Online
View Journal | View Issue

Cite this: *Polym. Chem.*, 2018, **9**, 1551

Received 3rd November 2017,
Accepted 10th January 2018

DOI: 10.1039/c7py01852e

rsc.li/polymers

Synthesis, aggregation and responsivity of block copolymers containing organic arsenicals†

Joji Tanaka,[a] Seiji Tani,[a] Raoul Peltier,[a] Emily H. Pilkington,[a,b] Andrew Kerr,[a] Thomas P. Davis[a,b] and Paul Wilson[*a,b]

Block copolymers containing an organic arsenical (AsAm) have been synthesised by aqueous SET-LRP. The block copolymers are pH and thermoresponsive, forming nanoparticles in aqueous solution. Under reductive conditions the particles are stabilised through the formation of As–As bonds and stability can be tuned as a function of the AsAm monomer feed.

Living systems crosslink (bio)macromolecules in order to stabilise intra- and intermolecular interactions, supporting complex tertiary and quaternary structures and self assembled (bio)macromolecular complexes. Such biochemical processes have inspired the development of a chemical platform to control the properties and function of polymers through crosslinking. Crosslinking synthetic linear polymers not only alters physical properties such as glass transition temperature, it has been exploited to create architectures beyond one dimensional linear structures such as single chain nanoparticles,[1,2] star/branched polymers,[3,4] and nanogels.[5] In particular, responsive materials that utilise reversible covalent bond formation that can be uncrosslinked on demand by specific environmental triggers are attractive targets for drug delivery, sustainability and chemical sensors.[6] In a biological context, boronate esters have been demonstrated by Sumerlin *et al.* as a pH and sugar responsive cross-linker to form hydrogels,[7,8] with self-healing properties in acidic environment, and self-assembled particles that dissemble in presence of sugars.[9–11] Other types of dynamic cross-linking such as hydrazones[12,13] and disulfides[14,15] are reported in the literature for intracellular drug delivery in response to endosomal pH and redox environment.

Arsenic is an interesting candidate for dynamic crosslinking, due to its interchangeable oxidation states each with distinct chemical reactivity. For example, pentavalent arsenic (As(v)) will not form covalent bonds with thiols, preferring to undergo single electron transfer reduction. Trivalent arsenic (As(III)) can be formed from the reduction of As(v) by two equivalents of thiol and in this oxidation state arsenic has a high affinity for thiols, readily forming covalent As–S bonds, which is markedly enhanced for dithiol reagents.[16] The affinity for mono- and dithiols has been exploited for post-polymerisation modification and protein/peptide-polymer conjugation of As-functional polymer scaffolds.[17,18] Under stronger reducing conditions, As(v) can be directly reduced to As(I), which has been reported to proceed with reductive coupling to form As_n homocycles comprised of As–As bonds.[19] The As–As bonds are weak but have been exploited in synthesis for the preparation of salvarsan[20] and as a source of monomer for 'ring-collapsed radical alternating copolymerisation' to form poly(vinylene arsines).[21–25]

Until recently, the polymerisation of As-functional monomers by chain-growth polymerisation was only reported by free radical polymerisation.[26–30] The advent of reversible deactivation radical polymerisation (RDRP) techniques such as reversible addition–fragmentation chain-transfer (RAFT),[31] atom transfer radical polymerisation (ATRP)[32,33] and single electron transfer living radical polymerisation (SET-LRP)[34] enables exquiste control of chain-end functionality which has been harnessed for the synthesis of well-defined (multi)block copolymers.[35,36] In previous work, a protected As-functional monomer, prepared in a two-step synthesis from *p*-arsanilic acid, was employed to prepare As-functional homo- and copolymers by RAFT.[17] In order to access the interesting reactivity of the pendant As-functional groups, the resulting polymers require an additional post-polymerisation processing step to afford deprotection. It would be beneficial to develop a method through which an As-functional monomer could be incorporated into polymers without the need for the additional protection (monomer)–deprotection (polymer) steps.

Herein we report the synthesis of block copolymers containing an As(v)-functional monomer (AsAm) by aqueous SET-LRP. At elevated temperatures As(v)-functional nanoparticles are

[a]*Chemistry Department, University of Warwick, Library Road, CV4 7AL Coventry, UK. E-mail: p.wilson.1@warwick.ac.uk*
[b]*ARC Centre of Excellence in Convergent Bio-Nano Science and Technology, Monash Institute of Pharmaceutical Sciences, Monash University (Parkville Campus), 399 Royal Parade, Parkville, Victoria 3152, Australia*

†Electronic supplementary information (ESI) available. See DOI: 10.1039/c7py01852e

formed which, for the first time, are stabilised by crosslinking through the reductive coupling of As(v) to give As(i)$_n$. The stability of the resulting particles as a function of the AsAm monomer feed is also investigated in aqueous and model biologically solutions.

Poly(ethylene glycol) methyl ether acrylate (PEGA, M_n = 480 g mol^{-1}) and *N*-isopropylacrylamide (NIPAm) are hydrophilic monomers that have been successfully polymerised by aqueous SET-LRP previously. Therefore, PEGA was selected as the corona-forming block and NIPAm, with its ability to undergo phase transition at elevated temperatures (LCST = 32 °C), was selected as the core-forming block. For optimal chain extension and block efficiency, the PEGA blocks (DP$_{n,th}$ = 20) were synthesised first then chain extended with NIPAm (DP$_{n,th}$ = 80) *via* one-pot, sequential chain extension in accordance with previous work.[35] The incorporation of As-functionality was achieved by statistical copolymerisation of varying amounts of AsAm in either the PEGA or NIPAM block, whilst keeping the overall chain length of the polymer constant (DP$_n$ = 100, Scheme S1†).

Initially, a non-As functional control polymer PEGA$_{20}$-*b*-NIPAm$_{80}$ was synthesised, with homopolymerisation of PEGA in water complete within 15 min (>99% conv., $M_{n,SEC}$ = 11 800 g mol^{-1}, $Đ$ = 1.07). Addition of a deoxygenated aliquot of NIPAm then furnished the targeted block copolymer PEGA$_{20}$-*b*-NIPAm$_{80}$ (**P1**, 98% conv., $M_{n,SEC}$ = 25 400 g mol^{-1}, $Đ$ = 1.27, Fig. S1†). Arsenical monomer, 4-(*N*-acrylamido) phenylarsonic acid (AsAm, ESI†), was then incorporated into corona-/core-forming blocks by altering the monomer feed ratio of either the first block (PEGA$_{20\text{-}n}$-*co*-AsAm$_n$, **P2** n = 3, **P3** n = 5) or the chain extension (NIPAm$_{80\text{-}n}$-*co*-AsAm$_n$, **P4** n = 5, **P5** n = 10). Successful inclusion of AsAm into the block copolymer was confirmed by ^{1}H NMR with appearance of aromatic signals of AsAm (H$_{l,m}$, Fig. 1) at 7.5–7.7 ppm in addition to the signals corresponding to PEGA (H$_{g,i}$) and NIPAm (H$_{j,k}$). The relative integrals were translated into an experimental polymer composition which confirmed the desired increase in AsAm content as a function of the AsAm monomer feed ratio (Fig. S2 and Table S1†). Block copolymerisation was confirmed by SEC analysis (Fig. S3†) which showed a shift to higher molecular weight upon chain extension. Increasing the amount of AsAm in either block appeared to have a detrimental effect on the control of the polymerisation as indicated by deviations in theoretical ($M_{n,th}$) and experimental number average molecular weight ($M_{n,SEC}$) and higher dispersities (**P2–P5**, $Đ$ = 1.2–1.8) than expected from aqueous SET-LRP polymerisations (Table 1).

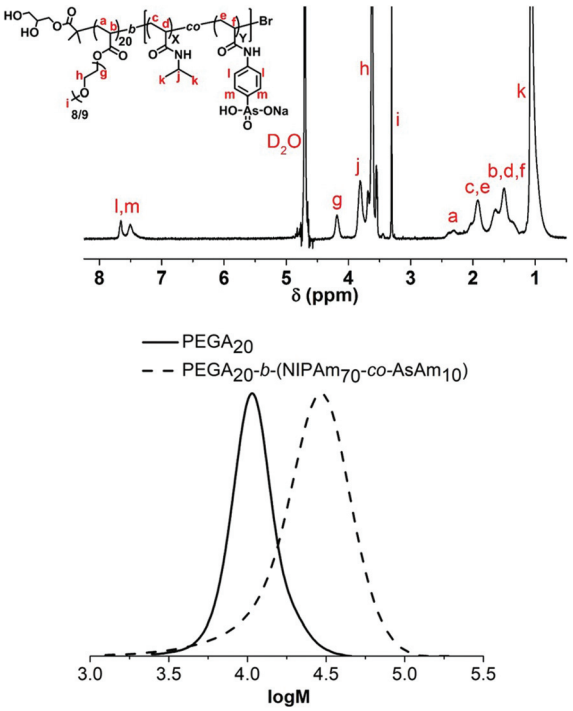

Fig. 1 Representative ^{1}H NMR (D$_2$O, top) and SEC (DMF, bottom) confirming the formation of As-functional block copolymers. SEC shows P(PEGA$_{20}$) $M_{n,th}$ = 9800 g mol^{-1}, $M_{n,SEC}$ = 10 100 g mol^{-1}, $Đ$ = 1.16 (solid) and PEGA$_{20}$-*b*-(NIPAM$_{70}$-*co*-AsAm$_{10}$) (**P5**); $M_{n,th}$ = 21 500 g mol^{-1}, $M_{n,SEC}$ = 26 000 g mol^{-1}, $Đ$ = 1.19 (dash).

The thermoresponsive behaviour and propensity for aggregation for each polymer was investigated by variable temperature dynamic light scattering (DLS) of aqueous solutions of the polymers (1 mg ml^{-1}) at 5 °C intervals between 25–60 °C. PNIPAm$_{80}$ synthesised by aqueous SET-LRP underwent macroscopic precipitation as expected between 35–40 °C (Fig. S4†),

Table 1 As-functional block copolymers synthesised by aqueous SET-LRP. ^{1}H NMR in D$_2$O. SEC in DMF

		First block				Final polymer			
Entry	Structures	Con.	$M_{n,th}$ (g mol^{-1})	$M_{n,SEC}$ (g mol^{-1})	$Đ$	Con.	$M_{n,th}$ (g mol^{-1})	$M_{n,SEC}$ (g mol^{-1})	$Đ$
Control									
P1	PEGA$_{20}$-*b*-NIPAm$_{80}$	>99%	9800	11 800	1.07	98%	20 000	25 400	1.27
P2	(PEGA$_{17}$-*co*-AsAm$_3$)-*b*-NIPAm$_{80}$	>99%	9200	11 100	1.51	>99%	19 400	25 100	1.41
P3	(PEGA$_{15}$-*co*-AsAm$_5$)-*b*-NIPAm$_{80}$	>99%	8800	16 500	1.29	>99%	19 000	37 500	1.81
P4	PEGA$_{20}$-*b*-(NIPAm$_{75}$-*co*-AsAm$_5$)	>99%	9800	7900	1.13	>99%	20 700	20 000	1.49
P5	PEGA$_{20}$-*b*-(NIPAm$_{70}$-*co*-AsAm$_{10}$)	>99%	9800	10 100	1.16	>99%	21 500	26 000	1.19
P6	PEGA$_{20}$-*b*-(NIPAm$_{65}$-*co*-AsAm$_{15}$)	>99%	9800	9200	1.18	>99%	22 200	21 000	1.42
P7	PEGA$_{20}$-*b*-(NIPAm$_{60}$-*co*-AsAm$_{20}$)	>99%	9800	9200	1.22	>99%	22 900	25 600	1.57

whereas the control block copolymer **P1** formed small aggregates with hydrodynamic diameters (D_h) of 12–15 nm at $T > 45$ °C (Fig. S5†).

Incorporation of AsAm into the corona-forming block also resulted in the formation of nanoparticles the size of which increased as a function of the AsAm monomer feed (**P2**, D_h = 20 nm; **P3**, D_h = 33 nm, Fig. S6†). However, when AsAm was incorporated into the core-forming NIPAm block (**P4** and **P5**) no self-assembly was observed (D_h = 4 nm, Fig. S7†). Under the reaction conditions the pendent arsenic acid group of AsAm is ionised (Na^+ salt) and hydrophilic. It was hypothesised that incorporation into the NIPAm block precluded the expected phase transition. Consequently, the pH of the polymer solutions was measured and found to be 10.3. Acidification of the polymer (**P4**) solution using HCl to close to neutral (pH = 6.6) had little effect resulting in no particle formation (D_h = 8 nm). However, further acidification to pH = 2.5, which is closer to the pK_a of arsenic acid (p$K_{a1} \approx 2$)[37] results in protonation of the arsenic acid groups leading to the formation of particles with D_h = 30 nm (Fig. S8†). In an identical titration, polymers **P2** and **P3** underwent self-assembly across the pH range forming nanoparticles, the sizes of which increased as the pH decreased (pH 10.3 = 48 nm; pH 2.5 = 98 nm, Fig. S8†).

In pure aqueous solution all the nanoparticles formed from **P1–P5** dissembled upon rehydration of the NIPAm block on cooling to 25 °C. Under reducing conditions (aqueous H_3PO_2), the pendent arsenic acid group (As(v)) can undergo reductive coupling to As(i),[19] with formation of As–As bonds in the form of As_n homocycles. It was hypothesised that reductive coupling could provide a novel approach to crosslinking and stabilisation of the organic arsenical copolymer nanoparticles derived from **P2–P5**. The polymers (10 mg ml^{-1}) were dissolved in an aqueous solution of H_3PO_2 prior to heating at 60 °C to facilitate both self-assembly and reduction processes. Under these conditions both **P2** and **P3** formed particles with D_h of the order of 40 nm and 80 nm respectively by DLS. However, the presence of the AsAm (n = 3, 5) in the corona-forming block was not sufficient to stabilise the particles formed after heating for 10–90 minutes, in line with previous methods employed to achieve reductive coupling.[20] Disassembly was observed within 10 minutes upon cooling back to 25 °C (Fig. S9†). Conversely, when AsAm was confined to the more densely packed core of the particles derived from **P4** (**NP_{As-5}**) and **P5** (**NP_{As-10}**), the particles formed (D_h = 45 nm) upon heating at 60 °C in the presence of H_3PO_2 retained their assembled structure upon cooling for up to 60 minutes, suggesting successful crosslinking through the formation of As–As bonds (Fig. S10†). The nature of the crosslinking was inferred from IR spectroscopy through disappearance of the As–O signals associated with the pendent arsenic acid (As(v)) moieties (Fig. S11†). Increasing the amount of AsAm in the monomer feed from **P4** (n = 5) to **P5** (n = 10) resulted in the formation of more stable particles, with **P5** forming stable particles after only 10 minutes of crosslinking, whereas **P4** required at least 30 minutes to form particles that were stable upon cooling to 25 °C (Fig. S12†).

The particles formed from **P5** (**NP_{As-10}**) exhibited thermoresponsive character, reversibly contracting and swelling upon heating and cooling cycles (Fig. S13†), in accordance with the transition of the core from a hydrophobic to hydrophilic state respectively. The enhanced stability of **NP_{As-10}** was further confirmed following purification and re-dispersion of the crosslinked particles in deionised water (1 mg ml^{-1}, Fig. S14†). Whereas **NP_{As-5}** was shown to disassemble during the purification process (dialysis against deionised water), **NP_{As-10}** retained its self-assembled structure and thermoresponsive properties (Fig. S15†). Transmission electron microscopy (TEM) and atomic force microscopy (AFM) of **NP_{As-10}** confirmed the formation of nanoparticles with sizes <100 nm (Fig. 2).

Two additional polymers were then synthesised to investigate the effect of AsAm monomer feed on self-assembly and particle stability. Thus, $PEGA_{20}$-*b*-$NIPAm_{80-n}$-*co*-$AsAm_n$ (**P6**, n = 15; **P7**, n = 20) were prepared. In line with the previous syntheses both blocks reached high conversion (>99%), the presence of each monomer was confirmed by ^{1}H NMR (Fig. S16†) and successful chain extension was confirmed by SEC analysis (Fig. S17†). The experimental monomer feed was again confirmed by ^{1}H NMR (Table S1†). This was supported by cryo-probe ^{13}C NMR which was performed to quantitiatively confirm the AsAm monomer feed ratio present in the block copolymers capable of forming self-assembled nanoparticles (**P4–P7**, Fig. S18 and Table S2†).

Polymers **P6** and **P7** underwent self-assembly in aqueous solution at elevated temperature (60 °C, Fig. S19†) and were cross-linked *via* reductive coupling, under the same conditions as **P5**. As expected, the resulting nanoparticles were sufficiently stabilised through reductive coupling to be re-dispersed in water, whereby the stabilised particles (**NP_{As-10}**, **NP_{As-15}**, **NP_{As-20}**) were analysed by DLS (Fig. S20†), TEM (Fig. S21†), and AFM (Fig. S22†). The data obtained for **NP_{As-15}** was in good agreement revealing particle sizes <50 nm whereas for **NP_{As-20}** DLS and AFM were in good agreement but the TEM revealed much larger particle sizes (≈200 nm). However, in the absence of staining with uranyl acetate, TEM of **NP_{As-20}** furnished smaller particles with sizes comparable to those obtained from DLS and AFM (Fig. S23†). To determine more accurate particle size data (radius of gyration – R_g, aggregation number – N_{agg} and nanoparticle molecular weight – $M_{w,NP}$) static light scattering (SLS) was performed (Fig. S24†). According to SLS particles **NP_{As-10}** and **NP_{As-15}** were similar, whereas increasing the AsAm monomer feed to n = 20 (**NP_{As-20}**) resulted in the formation of more densely packed particles as indicated by the increase in the $M_{w,NP}$ (1×10^6–4×10^6 g mol^{-1}) and N_{agg} (62–148), which coincided with a decrease in the D_h obtained from DLS (43–36 nm) (Table S3†).

The relative stabilities of **NP_{As-10}**, **NP_{As-15}** and **NP_{As-20}**, were initially investigated in aqueous solution at 37 °C, in which **NP_{As-10}** was found to be stable for 48 hours whereas **NP_{As-15}** and **NP_{As-20}** remained stable for at least 96 hours (Fig. S25†). In aqueous glutathione (GSH) at a concentration mimicking intracellular conditions ([GSH] = 5 mM), further differentiation in particle stability was observed. **NP_{As-10}** was stable for only 1 h with the majority of the nanoparticles undergoing disassem-

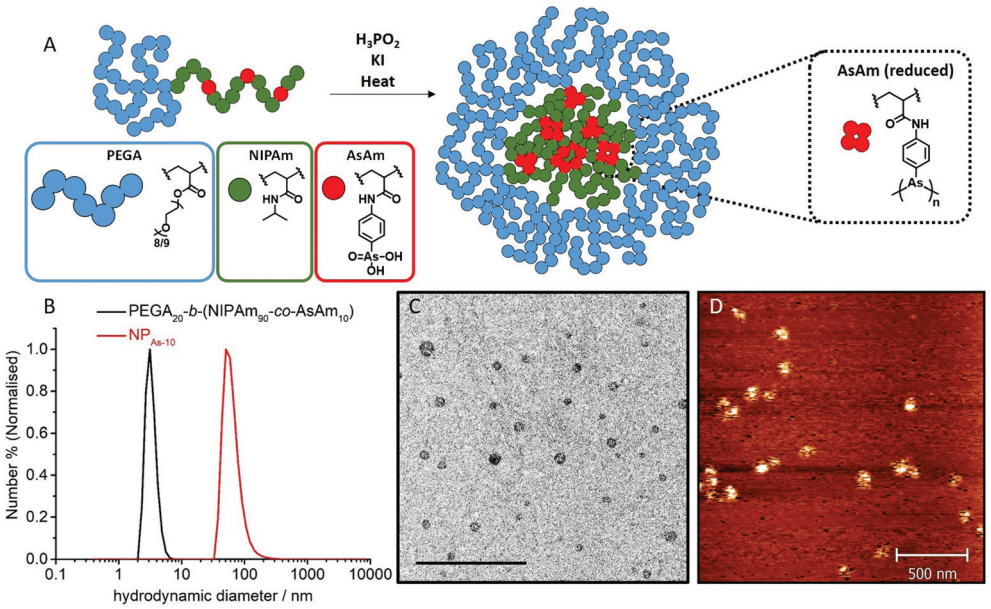

Fig. 2 (A) Schematic for the simultaneous self-assembly and reductive cross-linking of $PEGA_{20}$-*b*-($NIPAM_{70}$-*co*-$AsAm_{10}$) (**P5**) in H_3PO_2; (B) particle size distribution curves (DLS, 1 mg ml^{-1}, H_2O) of $PEGA_{20}$-*b*-($NIPAM_{70}$-*co*-$AsAm_{10}$) **P5** (black) and the corresponding crosslinked nanoparticle $\mathbf{NP_{As\text{-}10}}$ (red); (C) TEM image of $\mathbf{NP_{As\text{-}10}}$ (scale bar = 500 nm); (D) AFM image if $\mathbf{NP_{As\text{-}10}}$ (scale bar = 500 nm).

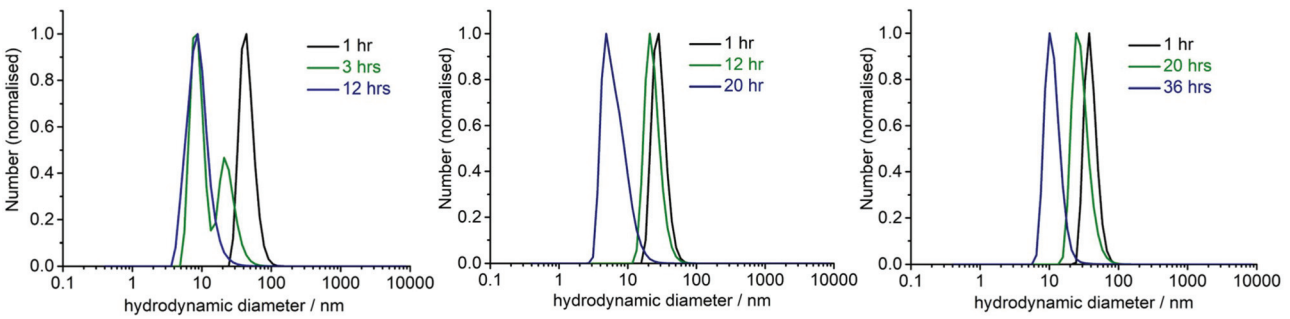

Fig. 3 Particle size distribution (DLS), illustrating the relative stability of $\mathbf{NP_{As\text{-}10}}$ (left), $\mathbf{NP_{As\text{-}15}}$ (centre) and $\mathbf{NP_{As\text{-}20}}$ (right) in aqueous GSH (5 mM, 1 mg ml^{-1}).

bly within 3 h. The enhanced rate of disassembly of $\mathbf{NP_{As\text{-}10}}$ was confirmed after incubation of $\mathbf{NP_{As\text{-}15}}$ and $\mathbf{NP_{As\text{-}20}}$ under identical conditions (5 mM GSH), which resulted in disassembly after 12 h and 20 h respectively (Fig. 3). Disassembly is attributed to the formation of more enthalpically favoured As–S bonds in favour of the weak As–As bonds originally formed through reductive coupling. The trend suggests that particle stability can be tuned by adjusting the AsAm monomer feed which could be advantageous for applications such as drug delivery. Finally, the stability was investigated under aggressive oxidative conditions (aqueous H_2O_2, 5 mM). Under these conditions all nanoparticles were completely disassembled within 1 h (Fig. S26†). As the particles were originally crosslinked *via* reductive coupling, it is likely that disassembly occurs under the strong oxidative conditions in aqueous solution through hydrolysis of the As–As bonds and oxidation of As(I) back to As(V).

Considering the successful synthesis, self-assembly and responsive crosslinking of As-functional block copolymers and with potential biomedical applications in mind, evaluation of their toxicity is essential. It has recently been reported that polymeric arsenicals exhibit limited toxicity *in vitro*.[17,18] Here, the acute toxicity of the As-functional block copolymers (**P2–P7**) and the nanoparticles ($\mathbf{NP_{As\text{-}10}}$, $\mathbf{NP_{As\text{-}15}}$, $\mathbf{NP_{As\text{-}20}}$) were determined *in vitro via* a standard XTT assay using the human PC3 cell line as model. PC3 (human prostate carcinoma) cells were obtained from the European Collection of Cell Cultures (ECACC). Pleasingly, it was found that all polymers (**P2–P7**) and their associated nanoparticles ($\mathbf{NP_{As\text{-}10}}$, $\mathbf{NP_{As\text{-}15}}$, $\mathbf{NP_{As\text{-}20}}$) were not toxic at concentrations up to 2.0 mg ml^{-1} (Fig. S27†).

Conclusions

Block copolymers containing an As-functional monomer (AsAm) have been synthesised by aqueous SET-LRP. Various amounts of AsAm have been incorporating into the hydro-

philic corona-forming block ((PEGA$_{20-n}$-*co*-AsAm$_n$)-*b*-NIPAm$_{80}$) or the thermoresponsive core-forming block (PEGA$_{20}$-*b*-NIPAm$_{80-n}$-*co*-AsAm$_n$). The block copolymers undergo self-assembly at elevated temperatures (60 °C) to form nanoparticles (D_h < 50 nm). Reductive coupling of pendent arsenic acid (As(v)) functional groups has been investigated for the first time for crosslinking and stabilisation. The presence of AsAm in the corona forming block (n = 3, 5) is insufficient for particle stabilisation upon cooling to ambient temperature. Conversely, incorporation of AsAm (n = 5, 10, 15, 20) into the more densely packed core of the nanoparticles affords particles that are stable upon cooling to ambient temperature. The nanoparticles and the polymers they are derived from are non-toxic and the stability of the nanoparticles in aqueous solution and model biological solutions (GSH, H_2O_2) increases as a function of the AsAm monomer feed, both of which we believe could be advantageous of biomedical applications.

Conflicts of interest

There are no conflicts to declare.

Acknowledgements

The authors gratefully acknowledge financial support from Engineering and Physical Sciences Research Council (EPSRC) under grant EP/F500378/1 through the Molecular Organisation and Assembly in Cells Doctoral Training Centre (MOAC-DTC) (J. T.). The authors also wish to acknowledge the facilities and personnel (T. P. D., E. P., P. W.) enabled by the Monash-Warwick Alliance. This work was carried out in conjunction with the Australian Research Council (ARC) Centre of Excellence in Convergent Bio-NanoScience and Technology (CE140100036). T. P. D. gratefully acknowledges support from the ARC in the form of an Australian Laureate Fellowship. P. W. thanks the Leverhulme Trust for the award of an Early Career Fellowship (ECF/2015-075). The authors would like to thank Dr Daniel Lester and the Polymer Characterisation Research Technology Platform for GPC facilities. The authors would like to thank Dr Ivan Prokes for running High resolution NMR and Dr Edward Mansfield for the help with setting up SLS.

Notes and references

1 J. Zhang, G. Gody, M. Hartlieb, S. Catrouillet, J. Moffat and S. Perrier, *Macromolecules*, 2016, **49**, 8933–8942.
2 J. Zhang, J. Tanaka, P. Gurnani, P. Wilson, M. Hartlieb and S. Perrier, *Polym. Chem.*, 2017, **8**, 4079–4087.
3 M. Hartlieb, T. Floyd, A. B. Cook, C. Sanchez-Cano, S. Catrouillet, J. A. Burns and S. Perrier, *Polym. Chem.*, 2017, **8**, 2041–2054.
4 C. Bray, R. Peltier, H. Kim, A. Mastrangelo and S. Perrier, *Polym. Chem.*, 2017, **8**, 5513–5524.
5 X. Zhang, S. Malhotra, M. Molina and R. Haag, *Chem. Soc. Rev.*, 2015, **44**, 1948–1973.
6 R. J. Wojtecki, M. A. Meador and S. J. Rowan, *Nat. Mater.*, 2011, **10**, 14–27.
7 J. J. Cash, T. Kubo, A. P. Bapat and B. S. Sumerlin, *Macromolecules*, 2015, **48**, 2098–2106.
8 C. C. Deng, W. L. A. Brooks, K. A. Abboud and B. S. Sumerlin, *ACS Macro Lett.*, 2015, **4**, 220–224.
9 D. Roy and B. S. Sumerlin, *ACS Macro Lett.*, 2012, **1**, 529–532.
10 A. P. Bapat, D. Roy, J. G. Ray, D. A. Savin and B. S. Sumerlin, *J. Am. Chem. Soc.*, 2011, **133**, 19832–19838.
11 D. Roy, J. N. Cambre and B. S. Sumerlin, *Chem. Commun.*, 2008, 2477–2479.
12 Z. Zhou, L. Li, Y. Yang, X. Xu and Y. Huang, *Biomaterials*, 2014, **35**, 6622–6635.
13 S. Binauld, W. Scarano and M. H. Stenzel, *Macromolecules*, 2012, **45**, 6989–6999.
14 H.-Y. Wen, H.-Q. Dong, W.-J. Xie, Y.-Y. Li, K. Wang, G. M. Pauletti and D.-L. Shi, *Chem. Commun.*, 2011, **47**, 3550–3552.
15 Y. Zhang, J. Zhou, C. Yang, W. Wang, L. Chu, F. Huang, Q. Liu, L. Deng, D. Kong, J. Liu and J. Liu, *Int. J. Nanomed.*, 2016, **11**, 1119–1130.
16 V. P. Whittaker, *Biochem. J.*, 1947, **41**, 56–62.
17 C. Footman, P. A. de Jongh, J. Tanaka, R. Peltier, K. Kempe, T. P. Davis and P. Wilson, *Chem. Commun.*, 2017, **53**, 8447–8450.
18 P. Wilson, A. Anastasaki, M. R. Owen, K. Kempe, D. M. Haddleton, S. K. Mann, A. P. Johnston, J. F. Quinn, M. R. Whittaker and P. J. Hogg, *J. Am. Chem. Soc.*, 2015, **137**, 4215–4222.
19 L. R. Smith and J. L. Mills, *J. Organomet. Chem.*, 1975, **84**, 1–15.
20 N. C. Lloyd, H. W. Morgan, B. K. Nicholson and R. S. Ronimus, *Angew. Chem., Int. Ed.*, 2005, **44**, 941–944.
21 K. Naka, T. Umeyama and Y. Chujo, *J. Am. Chem. Soc.*, 2002, **124**, 6600–6603.
22 T. Umeyama, K. Naka and Y. Chujo, *J. Polym. Sci., Part A: Polym. Chem.*, 2004, **42**, 3023–3028.
23 T. Umeyama, K. Naka and Y. Chujo, *J. Polym. Sci., Part A: Polym. Chem.*, 2004, **42**, 3604–3611.
24 T. Umeyama, K. Naka and Y. Chujo, *Macromolecules*, 2004, **37**, 5952–5958.
25 T. Umeyama, K. Naka, A. Nakahashi and Y. Chujo, *Macromolecules*, 2004, **37**, 1271–1275.
26 M. J. Percino, V. M. Chapela, R. Gutiérrez-Pérez and A. M. Herrera, *Des. Monomers Polym.*, 2000, **3**, 155–160.
27 T. Zayas, M. J. Percino, J. Cardoso and V. M. Chapela, *Polymer*, 2000, **41**, 5505–5512.
28 M. J. Percino, V. M. Chapela and A. Jiménez, *J. Appl. Polym. Sci.*, 2004, **94**, 1662–1669.
29 B. A. Yáñez-Martínez, J. Percino and V. M. Chapela, *J. Appl. Polym. Sci.*, 2010, **118**, 2849–2858.
30 G. Soriano-Moro, J. Percino, M. Cerón, M. E. Castro and V. M. Chapela, *J. Polym. Res.*, 2014, **21**, 492.

31 J. Chiefari, Y. K. Chong, F. Ercole, J. Krstina, J. Jeffery, T. P. T. Le, R. T. A. Mayadunne, G. F. Meijs, C. L. Moad, G. Moad, E. Rizzardo and S. H. Thang, *Macromolecules*, 1998, **31**, 5559–5562.
32 M. Kato, M. Kamigaito, M. Sawamoto and T. Higashimura, *Macromolecules*, 1995, **28**, 1721–1723.
33 J.-S. Wang and K. Matyjaszewski, *J. Am. Chem. Soc.*, 1995, **117**, 5614–5615.
34 A. Anastasaki, V. Nikolaou, G. Nurumbetov, P. Wilson, K. Kempe, J. F. Quinn, T. P. Davis, M. R. Whittaker and D. M. Haddleton, *Chem. Rev.*, 2016, **116**, 835–877.
35 F. Alsubaie, A. Anastasaki, P. Wilson and D. M. Haddleton, *Polym. Chem.*, 2015, **6**, 406–417.
36 G. Gody, T. Maschmeyer, P. B. Zetterlund and S. Perrier, *Nat. Commun.*, 2013, **4**, 2505.
37 S. A. Pergantis, *Analyst*, 1997, **122**, 1063–1068.